Communication

Carbon-nitrogen and nitrogen-nitrogen bond formation from nucleophilic attack at coordinated nitrosyls in Fe and Ru heme models

Erwin G. Abucayon, Douglas R. Powell, and George B. Richter-Addo

J. Am. Chem. Soc., **Just Accepted Manuscript** • Publication Date (Web): 24 Jun 2017

Carbon-nitrogen and nitrogen-nitrogen bond formation from nucleophilic attack at coordinated nitrosyls in Fe and Ru heme models

Erwin G. Abucayon, Douglas R. Powell, and George B. Richter-Addo*

Price Family Foundation Institute of Structural Biology and Department of Chemistry and Biochemistry, Stephenson Life Sciences Research Center, University of Oklahoma, Norman, OK 73019

Supporting Information Placeholder

ABSTRACT: The conversion of inorganic NOx species to organo-N compounds is an important component of the global N-cycle. Reaction of a *C*-based nucleophile, namely the phenyl anion, with the ferric heme nitrosyl $[(OEP)Fe(NO)(5\text{-}MeIm)]^+$ generates a mixture of the *C*-nitroso derivative (OEP)Fe(PhNO)(5-MeIm) and (OEP)Fe(Ph). The related reaction with $[(OEP)Ru(NO)(5\text{-}MeIm)]^+$ generates the (OEP)Ru(PhNO)(5-MeIm) product. Reactions with the *N*-based nucleophile diethylamide results in the formation of free diethylnitrosamine, whereas the reaction with azide results in N_2O formation; these products derive from attack of the nucleophiles on the bound NO groups. These results provide the first demonstrations of C–N and N–N bond formation from attack of *C*-based and *N*-based nucleophiles on synthetic ferric-NO hemes.

Nitric oxide (NO) is the simplest of the nitrogen oxides. It is an intermediate in denitrification as part of the global nitrogen cycle, being generated from nitrite reduction, and converted to nitrous oxide in a process involving N–N bond formation.[1-2] NO is also biosynthesized in mammals from enzymatic oxidation of L-arginine. An important reaction of NO in biology is its binding to heme Fe of the known receptor soluble guanylyl cyclase to regulate normal blood pressure in mammals.[3] Many other biological reactions of NO have been established, and these include enzyme inhibition,[4] oxidatively-induced modification of amino acid residues (e.g., cysteine nitrosation) to influence protein function,[5-6] and NO dioxygenase activity.[7]

A critical gap in knowledge exists, however, regarding the chemical steps in heme mediated modifications of NO to organo-NOx species. In fact, apart from (i) the well-studied hydroxide/alkoxide attack (and a preliminary study of azide attack) on the bound nitrosyls in ferric–NO hemes as part of reductive nitrosylation,[8-11] and (ii) hydride attack on ferric–NO heme models[12-13] or proton attack on reduced heme model-NO moieties[14-16] to generate Fe–HNO derivatives, very little is known regarding the chemistry of heme mediated generation of organo–NOx species from NO. This is somewhat surprising, given the fact the cytochrome cd_1 enzymes from denitrifying and non-denitrifying bacteria have been shown to catalyze, using nitrite, the nitrosation of organics such as morpholine in vitro and in vivo to generate carcinogenic nitroso compounds.[17-18] Such heme-based nitrosations during bacterial infections have been postulated to contribute towards some cancers in animals and humans.[17] In the observed heme-based nitrosations, the active nitrosating intermediates in these cyt cd_1 enzymes are proposed to be the electrophilic $[Fe^{3+}\text{–}NO \leftrightarrow Fe^{2+}\text{–}NO^+]$ species.[18-19] Interestingly, related nitrosations of *C*-based, *N*-based, and *S*-based organics have been demonstrated in vitro for the muscle protein myoglobin.[20]

It has been difficult to probe these heme-based nitrosation reactions, in large part due to the presumed instability of synthetic ferric–NO hemes. In fact, despite known examples of nucleophilic attack at bound nitrosyls in coordination and organometallic compounds,[21-23] it is surprising that there are no examples reported for biologically relevant ferric-NO heme models that generate new C–N and N–N bonds. We recently reported the synthesis of the elementally pure ferric nitrosyl [(OEP)Fe(NO)(5-MeIm)]OTf that is stable to NO dissociation in the solid state (≥4 months in air) and in solution (≥7 d under nitrogen) in the absence of added NO.[13] We showed that the coordinated nitrosyl in this and related ferric-NO heme compounds can be attacked by hydride to generate Fe–HNO derivatives.[12-13] We thus explored the possibility that the coordinated nitrosyl in

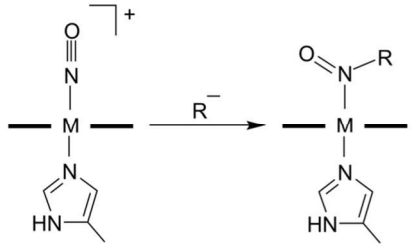

Figure 1. Attack of a *C*-based nucleophile on a coordinated nitrosyl in a heme model to generate a coordinated *C*-nitroso ligand.

[(OEP)Fe(NO)(5-MeIm)]OTf might also be susceptible to attack by *C*-based and *N*-based nucleophiles (e.g., Fig. 1). In this paper, we report the first demonstration of carbon-nitrogen and nitrogen-nitrogen bond formation mediated by synthetic ferric–NO porphyrins as models for biological heme-mediated nitrosations.

The reaction of [(OEP)Fe(NO)(5-MeIm)]OTf at 0 °C with 1.3 equiv. of PhLi in THF for 30 min results in a gradual change in color of the solution from red-purple to red. IR monitoring of the reaction shows the concurrent disappearance of the υ_{NO} band of the precursor at

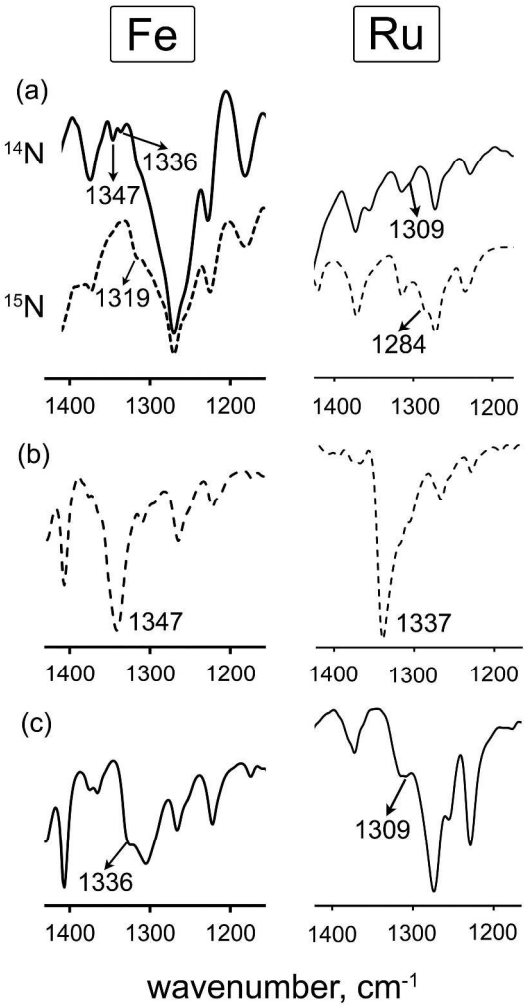

Figure. 2. IR spectra showing the formation of the (OEP)M(PhNO)(5-MeIm) products, as KBr pellets, for M = Fe (*left*) and M = Ru (*right*). (a) Formation of (OEP)Fe(PhNO)(5-MeIm) (υ_{NO} 1336 cm^{-1}) and (OEP)Fe(PhNO)$_2$ (υ_{NO} 1347 cm^{-1}) from the reaction of [(OEP)Fe(NO)(5-MeIm)]OTf with PhLi (*left*); and formation of the analogous (OEP)Ru(PhNO)(5-MeIm) (υ_{NO} 1309 cm^{-1}) product (*right*). The related spectra when the isotopic [(OEP)M(^{15}NO)(5-MeIm)]$^+$ compounds are used in the reactions are represented by the dotted lines. (b) IR spectra of independently synthetized (OEP)Fe(PhNO)$_2$ (*left*; formed in (a) above) and (OEP)Ru(PhNO)$_2$ (*right*; not formed in (a) above). (c) IR spectra of independently synthesized (OEP)Fe(PhNO)(5-MeIm) (*left*) and (OEP)Ru(PhNO)(5-MeIm) (*right*) using PhNO.

Table 1. Summary of the NO stretching frequencies of the (OEP)M(PhNO)(L) (M = Fe, Ru; L = 5-MeIm, 1-MeIm) products generated from reactions of the [(OEP)M(NO)(L)]$^+$ precursors with PhLi.

Compound	IR (KBr, cm^{-1})	
	υ_{NO}	υ_{15NO}
(OEP)Fe(PhNO)(5-MeIm)	1336	n.o.[a]
(OEP)Fe(PhNO)(1-MeIm)[b]	1337	n.o.[a]
(OEP)Fe(PhNO)$_2$	1346	1319
(OEP)Ru(PhNO)(5-MeIm)	1309	1284
(OEP)Ru(PhNO)(1-MeIm)	1306	1281

[a] Not observed; overlapping with porphyrin bands. [b] Previously reported in reference [24].

1912 cm^{-1} (NaCl plate), and the IR spectrum (Fig. 2a) of the resulting product mixture, obtained in ~50–55% total yield after work-up, as a KBr pellet revealed the formation of (OEP)Fe(PhNO)(5-MeIm) (υ_{NO} 1336 cm^{-1}; minor) and (OEP)Fe(PhNO)$_2$ (υ_{NO} 1347 cm^{-1}; minor),[25-26] and (OEP)Fe(Ph) ($\upsilon_{C\text{-}C}$ 1556 cm^{-1}; major)[27] that were difficult to separate (eq. 1).

$$[(OEP)Fe(NO)(5\text{-MeIm})]^+ \xrightarrow{Ph^-} \begin{matrix}(OEP)Fe(PhNO)(5\text{-MeIm}) \\ + \\ (OEP)Fe(PhNO)_2 + (OEP)FePh \\ + \textit{ other pdts}\end{matrix} \quad (1)$$

The spectral assignments of the mono- and bis-nitrosobenzene adducts (Table 1) were verified by the independent syntheses of (OEP)Fe(PhNO)$_2$ (Fig. 2b; left) and (OEP)Fe(PhNO)(5-MeIm) (Fig. 2c; left) (see Supporting Information). The analogous reaction of [(OEP)Fe(NO)(1-MeIm)]OTf with PhLi yielded a similar product mixture containing (OEP)Fe(PhNO)(1-MeIm) (υ_{NO} 1337 cm^{-1}),[24] (OEP)Fe(PhNO)$_2$, and (OEP)Fe(Ph). The formation of both the Fe–N(=O)Ph and Fe–Ph containing products demonstrates that the phenyl anion is capable of attacking both the nitrosyl N-atom and the Fe atom in these reactions.[28]

We extended this nucleophilic reaction to the congeneric Ru system. The reaction of [(OEP)Ru(NO)(5-MeIm)]BF$_4$ in THF at 0 °C with PhLi resulted in spectral changes indicative of the formation of a Ru–PhNO species (υ_{NO} 1309 cm^{-1}; υ_{15NO} 1284; Fig. 2a, right). The product with υ_{NO} 1309 cm^{-1} was isolated after workup that included column chromatography using neutral alumina, and was identified as (OEP)Ru(PhNO)(5-MeIm) (27% isolated yield) that was characterized by comparison of its IR spectral properties with those of an independently synthesized sample (Fig. 2c, right). We did *not* detect the formation of the (OEP)Ru(PhNO)$_2$ compound (υ_{NO} 1337 cm^{-1})[26] in this reaction. Importantly, the product with υ_{NO} 1309 cm^{-1} from the reaction of

[(OEP)Ru(NO)(5-MeIm)]BF_4 with PhLi was verified unambiguously as the (OEP)Ru(PhNO)(5-MeIm) derivative by single-crystal X-ray crystallography. The molecular structure is shown in Fig. 3, and clearly establishes that a new carbon-nitrogen bond has been formed from the phenyl attack at the linear nitrosyl ligand in the

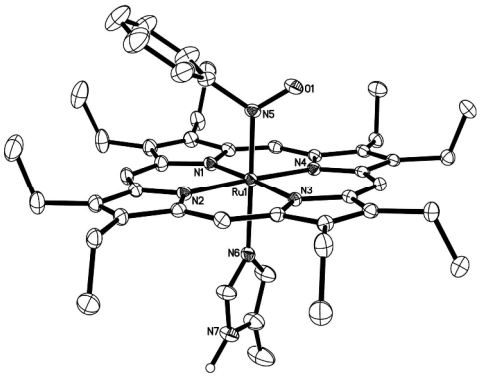

Figure. 3. Molecular structure of the product from the reaction of [(OEP)Ru(NO)(5-MeIm)]BF_4 with PhLi, revealing the identity of the PhNO ligand resulting from C–N bond formation. Thermal ellipsoids are shown at 50% probability (CCDC 1545442). The hydrogen atoms (except for the imidazole N7 proton) have been omitted for clarity. Selected bond lengths (in Å) and angles (°): Ru–N5 = 1.887(2), Ru–N6 = 2.123(2), ∠Ru–N5–O1 = 124.42(18), ∠Ru–N5–C = 123.00(17), ∠N5–Ru–N6 = 177.15(9).

precursor cation. The analogous reaction of [(OEP)Ru(NO)(1-MeIm)]OTf with PhLi also generated the (OEP)Ru(PhNO)(1-MeIm) derivative in 33% isolated yield. *This observed C-based nucleophilic attack at a bound nitrosyl ligand is unprecedented in heme model systems.*

We thus sought to explore if such nucleophilic attack could be extended to other *N*-nucleophiles. The reaction of [(OEP)Fe(NO)(5-MeIm)]OTf with $LiNEt_2$ in THF generates the free nitrosamine Et_2NNO (by ^{1}H NMR and GC-MS; Fig. S1) and (OEP)Fe(NO) (by IR), in 13% and 71% unoptimized yields, respectively.[29-31] The analogous reaction with [(OEP)Ru(NO)(5-MeIm)]BF_4 also yielded Et_2NNO, albeit in lower 8% unoptimized yield.

The reaction of 1.5 equiv. of NaN_3 with [(OEP)Fe(NO)(5-MeIm)]OTf in THF/DMF (4:1) solvent resulted in the generation of gaseous N_2O as determined by IR spectroscopy of the headspace gases. When [(OEP)Fe(^{15}NO)(5-MeIm)]OTf was used in this reaction, the IR spectrum of the headspace revealed bands at 2189 and 2165 cm^{-1} assigned to the formation of mixed N-isotope gaseous product $^{14}N^{15}NO$ (Fig. 4a);[32] we did not detect $^{15}N^{14}NO$ or either of the single N-isotope gases $^{15}N_2O$ or $^{14}N_2O$.[32] The analogous reaction of [(OEP)Ru(NO)(5-MeIm)]$^+$ with azide also resulted in the generation of N_2O. However, when the ^{15}N-labeled [(OEP)Ru(^{15}NO)(5-MeIm)]$^+$ was used in this reaction, both singly-labeled $^{14}N^{15}NO$ and unlabeled $^{14}N_2O$ were generated (Fig. 4b).

The generation of the single $^{14}N^{15}NO$ product when the Fe–^{15}NO reagent is used, but both $^{14}N^{15}NO$ and $^{14}N^{14}NO$ when the Ru–^{15}NO reagent is used, suggests different intermediates. The Fe case is reminiscent of the products obtained when azide reacts with cyt cd_1[18-19] or nitroprusside,[33] and strongly suggests an intermediate of the form "Fe–^{15}N(=O)NNN" containing a coordinated linear nitrosyl azide.[34-35] In contrast, the generation of both $^{14}N^{15}NO$ and $^{14}N_2O$ in the case of Ru suggests an

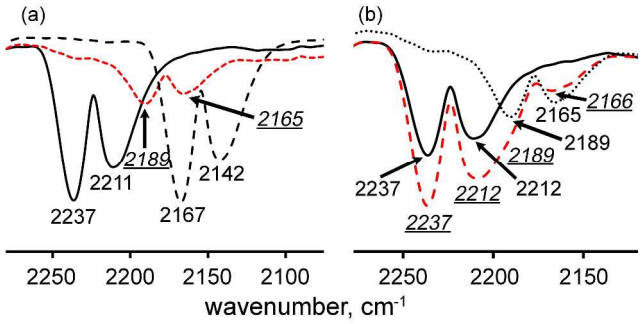

Figure 4. (a) The gas-phase IR spectrum of the headspace collected from the reaction of [(OEP)Fe(^{15}NO)(5-MeIm)]OTf with azide shows bands at 2189/2165 cm^{-1} (*red dotted line*) characteristic of the $^{14}N^{15}NO$ isotopomer. IR spectra of unlabeled N_2O (2237/2211 cm^{-1}; *solid line*) and doubly labeled $^{15}N_2O$ (2167/2142 cm^{-1}; *dashed line*) are also shown for reference.[32] (b) The gas-phase IR spectrum from the reaction of [(OEP)Ru(^{15}NO)(5-MeIm)]BF_4 with azide (*red broken line*) shows bands at 2237/2212 cm^{-1} (major) and 2189/2165 cm^{-1} (minor) due to unlabeled N_2O and labeled $^{14}N^{15}NO$, respectively. IR spectra of unlabeled N_2O (2237/2211 cm^{-1}; *solid line*) and singly labeled $^{14}N^{15}NO$ (2189/2168 cm^{-1}; *dotted line*) are also shown for reference.

intermediate with a cyclic N_4O contribution that decomposes via the two paths shown in Fig. 5, where cleavage of bonds 1 and 3 in this intermediate would generate the unlabeled $^{14}N_2O$, whereas cleavage of bonds 3 and 5 would generate the singly labeled $^{14}N^{15}NO$.[35-38] That the

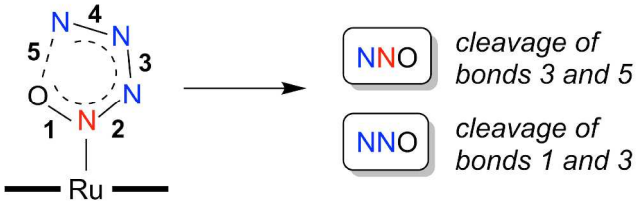

Figure 5. Proposed pathway for the production of labeled and unlabeled N_2O mediated by the Ru heme model.

$^{14}N_2O$ (major) and $^{14}N^{15}NO$ (minor) gases are formed in unequal amounts suggests a decomposition while the N_4O is still bound to Ru, as dissociation of N_4O prior to decomposition should give equal amounts of $^{14}N_2O$ and $^{14}N^{15}NO$.

In summary, we provide the first demonstration of nucleophilic attack of *C*-based and *N*-based nucleophiles at the electrophilic nitrosyls in ferric-NO heme models to

generate new C–N and N–N bonds. These reactions are of relevance to the study of biological nitrosations carried out by heme enzymes.

ASSOCIATED CONTENT

Supporting Information.
The Supporting Information is available free of charge via the Internet at http://pubs.acs.org.

Experimental, crystallographic data, additional figure (PDF)

AUTHOR INFORMATION

Corresponding Author: grichteraddo@ou.edu

Notes
The authors declare no competing financial interest.

ACKNOWLEDGMENTS

We are grateful to the National Science Foundation (CHE-1566509 to GBRA) and for a Nancy Mergler Dissertation Completion Fellowship from the University of Oklahoma (to EGA) for funding for this work.

REFERENCES

1. Eady, R. R.; Hasnain, S. S., Denitrification. In *Comprehensive Coordination Chemistry II*, Que Jr., L.; Tolman, W. B., Eds. Elsevier: San Diego, CA, 2004; Vol. 8 (Bio-coordination chemistry), pp 759-786.
2. Wasser, I. M.; de Vries, S.; Moenne-Loccoz, P.; Schroder, I.; Karlin, K. D., *Chem. Rev.* **2002,** *102*, 1201-1234.
3. Herzik, M. A.; Jonnalagadda, R.; Kuriyan, J.; Marletta, M. A., *P Natl Acad Sci USA* **2014,** *111*, E4156-E4164.
4. Stadler, J.; Schmalix, W. A.; Doehmer, J., *Adv. Exptl. Med. Biol.* **1996,** *387*, 187-193.
5. Zhang, R. L.; Hess, D. T.; Reynolds, J. D.; Stamler, J. S., *J Clin Invest* **2016,** *126*, 4654-4658.
6. Anand, P.; Stamler, J. S., *J. Mol. Med.* **2012,** *90*, 233-244.
7. Gardner, P. R., *J. Inorg. Biochem.* **2005,** *99*, 247-266.
8. Ford, P. C.; Fernandez, B. O.; Lim, M. D., *Chem. Rev.* **2005,** *105*, 2439-2455.
9. Hoshino, M.; Maeda, M.; Konishi, R.; Seki, H.; Ford, P. C., *J. Am. Chem. Soc.* **1996,** *118*, 5702-5707.
10. Azide has been shown to greatly enhance the rate of reduction of water-soluble $(TPPS)Fe^{III}$ by NO, presumably via azide attack on the bound nitrosyl in $(TPPS)Fe^{III}(NO)$.[11]
11. Fernandez, B. O. Ph.D. Thesis, University of California Santa Barbara, 2004. Cited in Section 3.4 of reference 8.
12. Abucayon, E. G.; Khade, R. L.; Powell, D. R.; Shaw, M. J.; Zhang, Y.; Richter-Addo, G. B., *Dalton Trans.* **2016,** *45*, 18259-18266.
13. Abucayon, E. G.; Khade, R. L.; Powell, D. R.; Zhang, Y.; Richter-Addo, G. B., *J. Am. Chem. Soc.* **2016,** *138*, 104-107.
14. Goodrich, L. E.; Roy, S.; Alp, E. E.; Zhao, J. Y.; Hu, M. Y.; Lehnert, N., *Inorg. Chem.* **2013,** *52*, 7766-7780.
15. Liu, Y.; Ryan, M. D., *J. Electroanal. Chem.* **1994,** *368*, 209-219.
16. Rahman, M. H.; Ryan, M. D., *Inorg. Chem.* **2017,** *56*, 3302-3309.
17. Calmels, S.; Ohshima, H.; Henry, Y.; Bartsch, H., *Carcinogenesis* **1996,** *17*, 533-536.
18. Kim, C.-H.; Hollocher, T. C., *J. Biol. Chem.* **1984,** *259*, 2092-2099.
19. Goretski, J.; Hollocher, T. C., *Biochem. Biophys. Res. Commun.* **1991,** *175*, 901-905.
20. Wade, R. S.; Castro, C. E., *Chem. Res. Toxicol.* **1990,** *3*, 289-291.
21. Bottomley, F., Reactions of Nitrosyls. In *Reactions of Coordinated Ligands*, Braterman, P. S., Ed. Plenum Press: New York, 1989; Vol. 2, pp 115-222.
22. Xu, N.; Richter-Addo, G. B., *Prog. Inorg. Chem.* **2014,** *59*, 381-445.
23. Doctorovich, F.; Di Salvo, F., *Acc. Chem. Res.* **2007,** *40*, 985-993.
24. Godbout, N.; Sanders, L. K.; Salzmann, R.; Havlin, R. H.; Wojdelski, M.; Oldfield, E., *J. Am. Chem. Soc.* **1999,** *121*, 3829-3844.
25. The $(OEP)Fe(PhNO)_2$ compound is in equilibrium with the mononitrosobenzene compound (OEP)Fe(PhNO) in solution; as observed previously for $(OEP)Ru(PhNO)_2$.[26]
26. Crotti, C.; Sishta, C.; Pacheco, A.; James, B. R., *Inorg. Chim. Acta* **1988,** *141*, 13-15.
27. Guilard, R.; Boisselier-Cocolios, B.; Tabard, A.; Cocolios, P.; Simonet, B.; Kadish, K. M., *Inorg. Chem.* **1985,** *24*, 2509-2520.
28. Interestingly, we find that the reactions of [(OEP)Fe(NO)(5-MeIm)]OTf with the arylating agents PhMgX (X = Cl, Br) resulted in the formation of (OEP)Fe(NO)(Ph) at 0 °C, or (OEP)Fe(Ph) at room temperature (data not shown), with no evidence of nucleophilic attack at the nitrosyl N atom under our reaction conditions.
29. We have previously shown that nitrosamines can bind directly to ferric heme models, and that arylnitrosamines can nitrosylate ferrous heme models to give (por)Fe(NO).[30] Conversely, *ferrous* (por)Fe(NO) can nitrosate amines to give nitrosamines.[31]
30. Xu, N.; Goodrich, L.; Lehnert, N.; Powell, D. R.; Richter-Addo, G. B., *Inorg. Chem.* **2010,** *49*, 4405-4419.
31. Bonnett, R.; Charalambides, A. A.; Martin, R. A., *J. Chem. Soc., Perkin Trans. 1* **1978**, 974-980.
32. Dubowski, Y.; Harush, D.; Shaviv, A., *Soil Sci. Soc. Am. J.* **2014,** *78*, 61-69.
33. Wolfe, S. K.; Andrade, C.; Swinehart, J. H., *Inorg. Chem.* **1974,** *13*, 2567-2572.
34. The *trans* isomer of free ONN_3 is calculated to be ~1 kcal/mol more stable than the *cis* isomer.[35]
35. Schulz, A.; Tornieporthoetting, I. C.; Klapotke, T. M., *Angew. Chem. Int. Ed.* **1993,** *32*, 1610-1612.
36. The cyclic N_4O isomer in the free state has been calculated to be 13 kcal/mol more favorable than the linear *trans* isomer.[35]
37. Such a cyclic N_4O intermediate has been suggested for a coordination compound of Ru.[38]
38. Douglas, P. G.; Feltham, R. D., *J. Am. Chem. Soc.* **1972,** *94*, 5254-5258.

.

Insert Table of Contents artwork

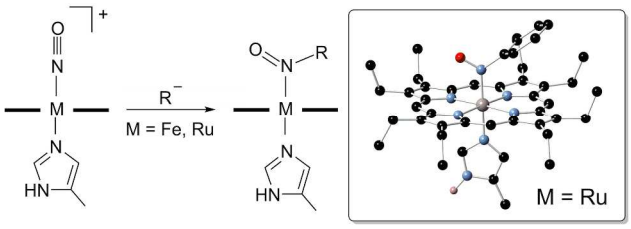

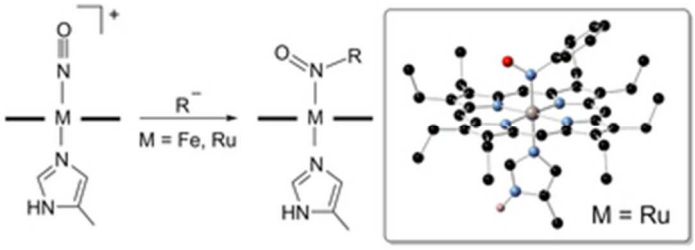

Table of Contents graphic

29x10mm (300 x 300 DPI)

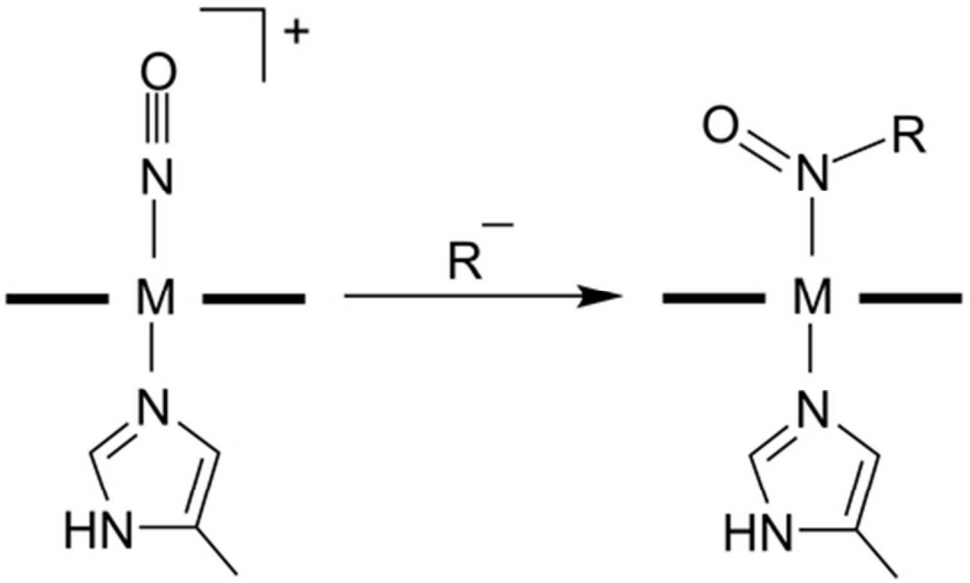

Figure 1

41x25mm (300 x 300 DPI)

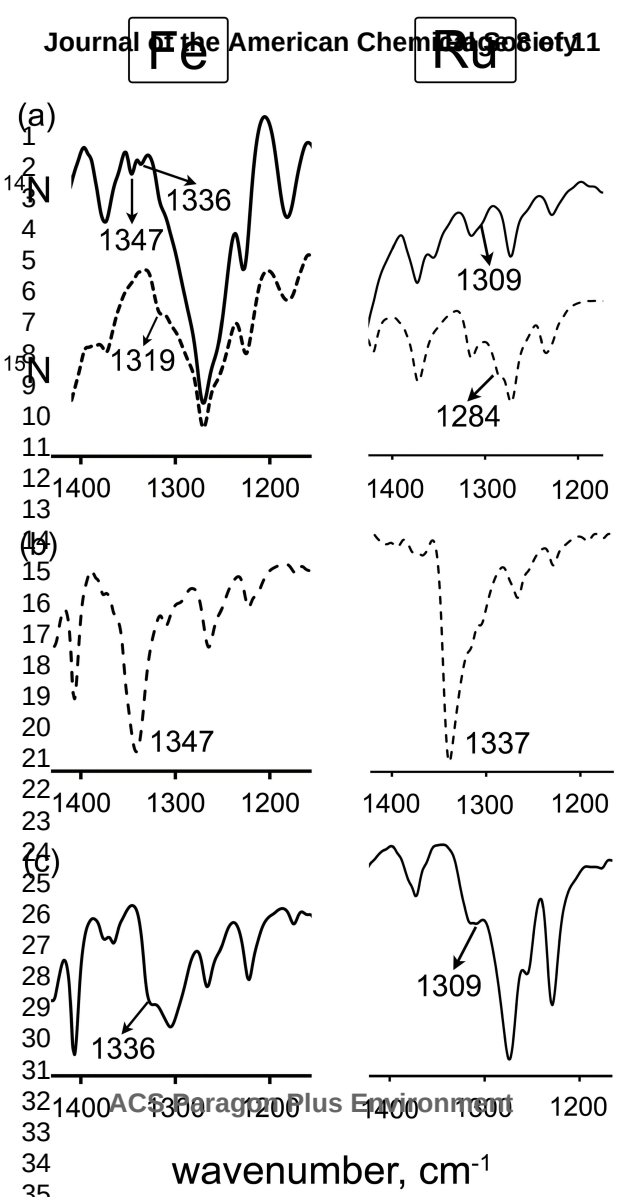

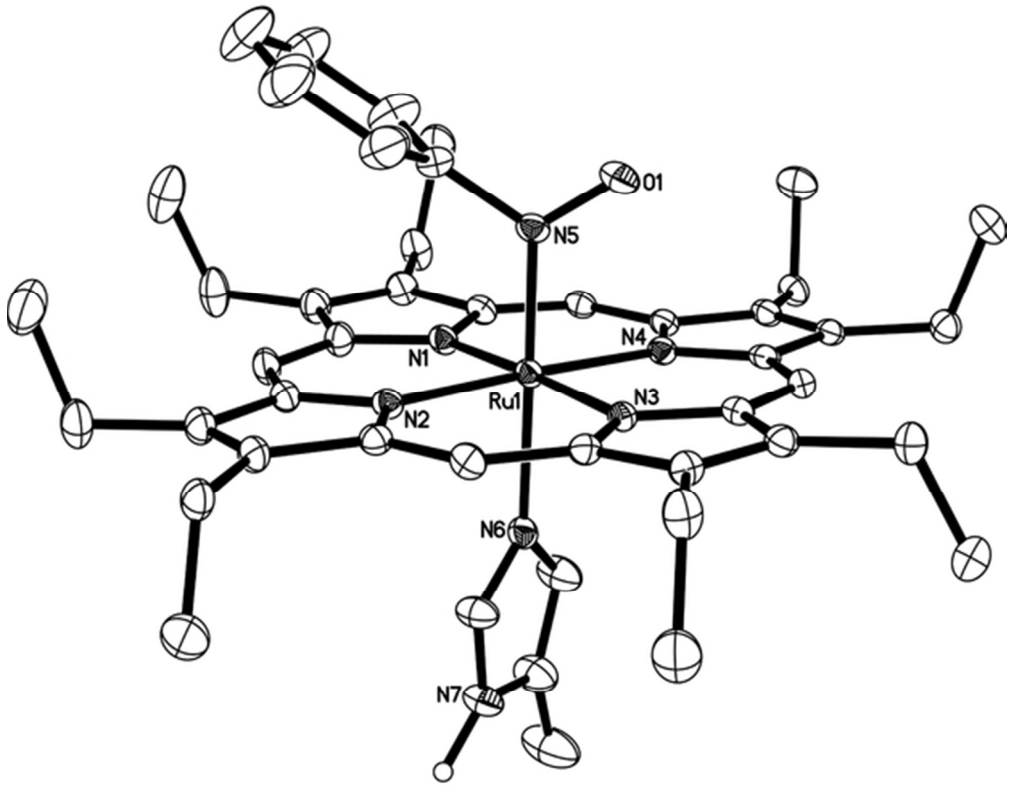

Figure 3

52x41mm (300 x 300 DPI)

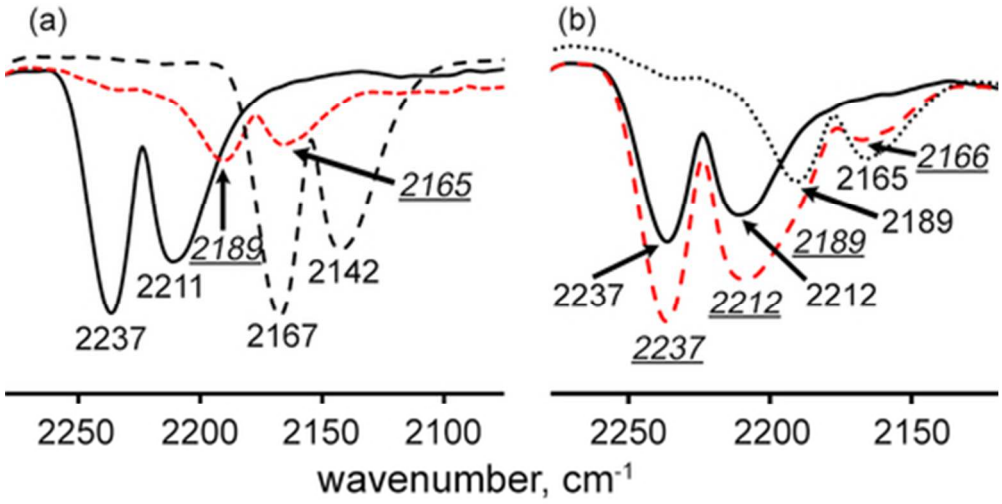

Figure 4

41x21mm (300 x 300 DPI)

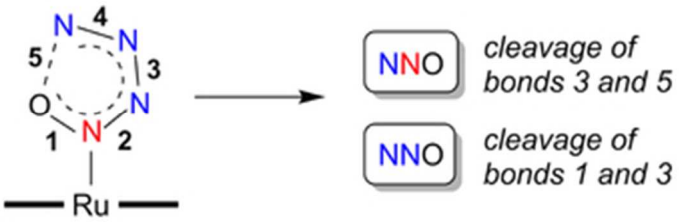

Figure 5

28x9mm (300 x 300 DPI)